

FIRST YEAR'S OPERATION OF THE CHALK RIVER SUPERCONDUCTING CYCLOTRON

J.A. Hulbert, C.B. Bigham, W.G. Davies, B.F. Greiner, E.A. Heighway\*, J.D. Hepburn, C.R.J. Hoffmann, E.H. Lindqvist, J.H. Ormrod, E.P. Stock and L.W. Thomson  
 Atomic Energy of Canada Limited, Research Company  
 Chalk River Nuclear Laboratories, Chalk River, Ontario, Canada K0J 1J0

Summary

The Chalk River Superconducting Cyclotron has now been in operation for one year. The cyclotron is described and the progress in commissioning outlined. Some details are given on special features of the machine, including injection, isochronizing and extraction. Typical beam properties are listed and the remaining commissioning tasks before the cyclotron achieves full specification are summarized.

Introduction

The Chalk River superconducting cyclotron first accelerated beam one year ago. A number of nuclear physics experiments have been carried out with the extracted beam and work is continuing to commission the machine to its full capability. The innovative concepts in the machine design have proven successful and beam development has been straightforward using the predictions of beam dynamics orbit codes.

Description of the Cyclotron

The plan of the TASCC (Tandem Accelerator Superconducting Cyclotron) facility is shown in Fig. 1. Negative ions are generated in the 300 kV ion injector and accelerated to the terminal of the 13 MV MP tandem. In preparation for injection into the cyclotron (Fig. 2) the beam is bunched in the gridded-gap prebuncher, which contains two cavities tuned to the cyclotron fundamental and 2nd harmonic frequencies, to approximate a saw-tooth waveform at the grid. The bunches reach a time focus at the tandem stripper canal to minimize the effects of energy spread from straggling. The stripped beam accelerated from the tandem terminal passes through an analyzing dipole.

The injection beam line to the cyclotron<sup>1</sup> consists of three achromatic sets of magnets. Three quadrupole lenses in the cyclotron matching system are adjustable in axial position to enable the injected beam, over the full range of ion masses and energies, to be varied in magnification and matched to the admittance and dispersive properties of the cyclotron. A drift tube harmonic buncher located between the first two dipole pairs, rebunches the beam to give a time focus at a foil, which, located at a variable radius inside a cyclotron dee strips the incoming beam for injection into the first concentric orbit. Figure 3 shows a mid-plane section of the cyclotron.

A set of four injection steering magnets determines the direction from which an incoming beam passes the common injection point, near the outer wall of the cryostat. The injection energy, initial charge state, injection angle and stripper foil radius are then determined by the isochronous field distribution and final charge state required for the selected extracted ion and energy. The required ranges and some typical values are given in Table 1.

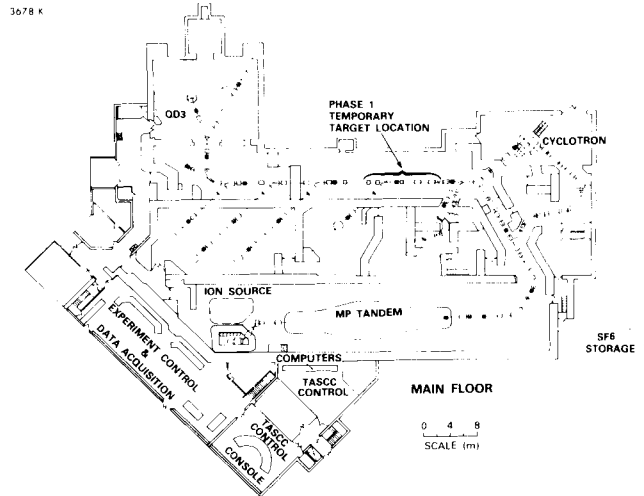


Fig. 1 The Chalk River Tandem Accelerator Superconducting Cyclotron (TASCC) facility.

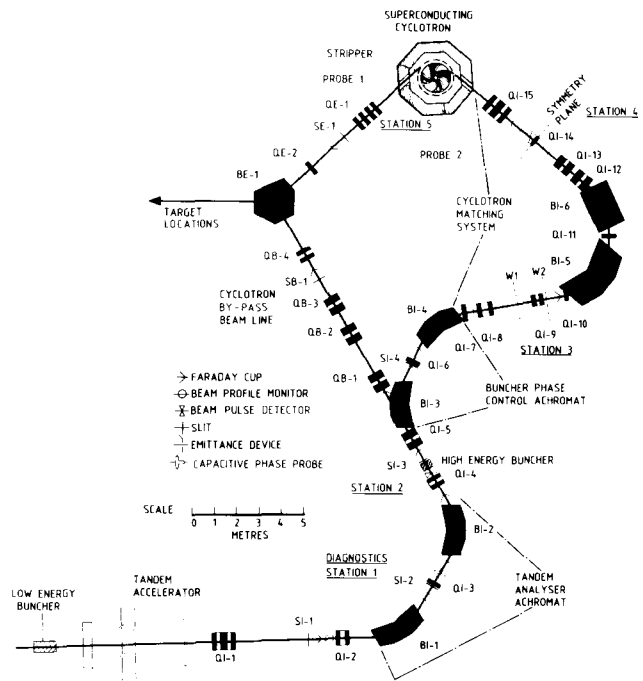


Fig. 2 Injection and extraction beam line of the Chalk River Superconducting Cyclotron.

\*Present address: Los Alamos National Laboratory, Los Alamos, New Mexico, U.S.A.

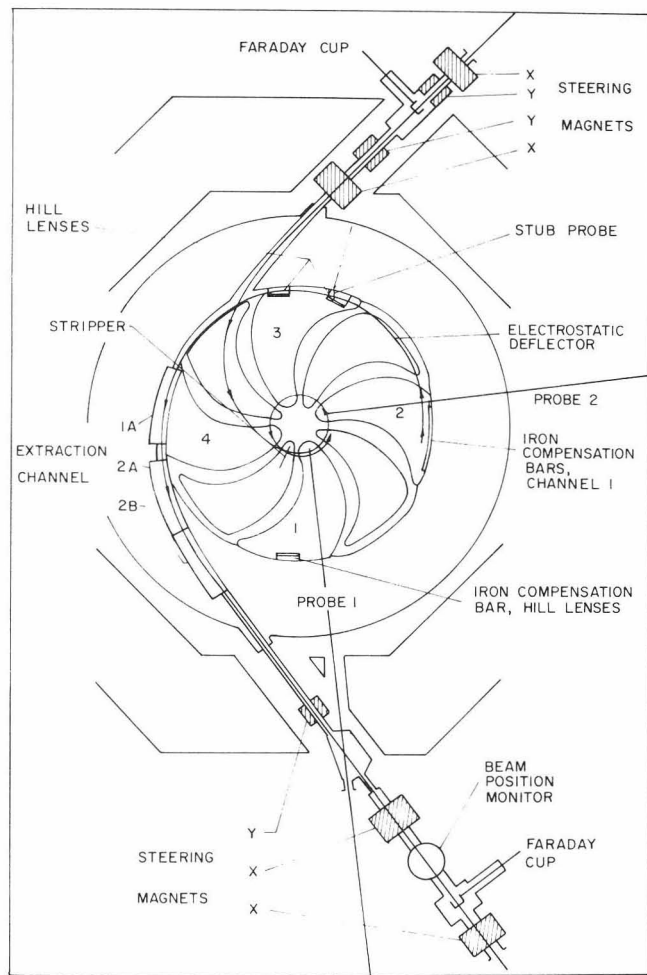


Fig. 3 Midplane section of the Chalk River Superconducting Cyclotron.

Two radial probes, which move along paths between magnetic hills 1 and 2 respectively are used to track the turn pattern of the accelerated beam orbits out to the extraction radius at 650 mm. Axial and radial beam position information from these probes is used to adjust the rf phase and orbit centering.

A first harmonic magnetic field distribution is established at the outer radii to decentre the beam orbit and direct the beam into the entrance of the electrostatic deflector, which steers the beam into the entrance of the magnetic extraction channel. Two saturated iron gradient lenses maintain radial focusing between deflector and magnetic channel. In channel section 1, superconducting windings bias the axial magnetic field while saturated iron bars maintain the radial focusing gradient. Channels 2A and 2B have independent superconducting bias windings and series-connected superconducting gradient windings powered by three separate current supplies. Fields from the extraction system are compensated in the acceleration region by superconducting compensating windings incorporated in the channel and the saturated iron compensating bars shown in Fig. 3. The beam position and profile after extraction may be measured by withdrawing Probe 1 to the location at the outer edge of the magnet yoke.

Table 2 shows the principal parameters of the cyclotron.

Table 1

	Injection Conditions		Foil Radius mm	Injection Energy MeV	Steering Angle degrees
	Charge State Before Strip	Charge State After Strip			
$^{127}\text{I}$ , 10 MeV/u	7	23	151.0	70.89	+0.04
$^{127}\text{I}$ , 5.6 MeV/u	6	19	154.5	42.07	+0.006
$^{127}\text{I}$ , 5.12 MeV/u	6	18	166.3	44.17	-0.173
$^{78}\text{Br}$ , 20 MeV/u	6	20	149.0	84.69	+0.112
Range	1-10	3-33	145-265	4.4-143	$\pm 2.0$

Calendar

At the time of the last Cyclotron Conference at East Lansing (May 1984) the cyclotron was being prepared for its removal from the development laboratory to its final location in its shielded vault. Table 3 gives the chronology of the final assembly and commissioning.

After the East Lansing conference, the isochronous field was set for  $^{127}\text{I}$ , 10 MeV/u, the commissioning ion and the field mapped. Following the mapping, no changes were made to the trim rod settings until after the successful acceleration of the commissioning ion.

When the rf power was turned on for the first attempt at acceleration it became apparent that the demountable joints at the bases of the main tuners had not survived the development tests and subsequent transportation without distortion and consequent vacuum leakage. The poles were removed, the joint seals (vacuum and rf) taken out and the joints brazed permanently.

Table 2

The Chalk River Superconducting Cyclotron

Magnet Poles:	Compact, four spiral sectors (50° maximum spiral angle) Diameter 1386 mm Injection radius 145-265 mm Extraction radius 650 mm Pole gap (including copper facing) 34 mm in hills 640 mm in valleys
Magnet Coil:	Superconducting Nb-Ti, 25:1 copper:superconductor 6.2 x 10 <sup>6</sup> Ampere-turns maximum Weight 10 tonnes (18 tonnes with cryostat) Operating temperature 4.6 K
Injector:	MP Tandem 13 MV maximum
Ion Energy Limits:	Bending 520 q <sup>2</sup> /a MeV Focusing 100 q/a MeV Ions accelerated Li (50 MeV/u max) to U (10 MeV/u max)
Accelerator System:	4 dees 100 kV maximum rf frequency 31-62 MHz harmonics used 2, 4, 6
Field Trimming:	Coil divided into outer and inner coil pairs separately excited. 13 saturated iron trim rods in each flutter pole, 104 in all, positioned by stepping motor geared drives.

Once the rf was operating at the required power level, development of the accelerated beam to the extraction radius took only three days. The magnetic field was set according to beam dynamics calculations and then changed by an increase of 0.04% to obtain isochronism. Progress to extraction was first delayed by the need to install the electrostatic deflector and complete the assembly of the extraction beam line, and by problems with the helium liquefier. Beam was first extracted on November 19. When the beam was guided into the magnetic channel an operational problem of superconducting magnetic channels become apparent. Despite precautions, ice had condensed in the channel beam pipe while the lower pole was being raised and its seal closed. On occasion the ice completely stopped the beam until melted by beam power, but all extracted beams showed bifurcation due to stripping. After some trials, a beam pipe bakeout heater was developed which could be inserted into the beam pipe under vacuum. It is now routine to bake out the extraction beam pipe overnight after each occasion when the midplane is opened to atmosphere. A stable beam, showing no indication of stripping in the extraction beam pipe was extracted on 1986 February 10 and a 20 nA beam of  $^{127}\text{I}$ , 10 MeV/u delivered to the experimental target location on February 21.

The second beam required for physics experiments was  $^{127}\text{I}$  at 5.1 MeV/u. This beam is located, in the energy-mass plane, just inside the boundary for the 6th harmonic  $\pi$ -mode of excitation of the rf structure, as shown in Fig. 4. In the  $\pi$ -mode, in which adjacent dees are excited with opposite polarity, rf currents flow azimuthally across the dee faces and around the cryostat wall. These currents induce strong heating in the diagnostic probes sleeves and on extraction elements and round probe ports in the cryostat wall. Further, probe motion causes appreciable cavity de-tuning. Cooling in the original probe design was inadequate to cope with the  $\pi$ -mode heating and the probes have been redesigned to provide better cooling. The detuning effects can be compensated by using the two rf balance capacitors, located in two lower valleys, to augment the range of the fine tuner. Remodeling of the rf wall shielding round the hot spots on the cryostat wall is awaiting the next midplane opening, scheduled for 1986 December, and until then the rf structure is restricted to 0-mode operation.

By going to 5.6 MeV/u, it is possible to use the 0-mode near the low frequency limit, and two experiments have been performed with that beam.

A 20 MeV/u,  $^{79}\text{Br}$  beam is being developed this month, which moves the operating point to 59.9 MHz, near the highest frequency of the rf system (62 MHz). RF operating tests at 59.5 MHz revealed a vacuum problem which at present limits us to a dee voltage of 50 kV at this frequency. Until this problem is overcome development of the Br beam will be possible only with a high number of turns. For  $^{79}\text{Br}^{20+}$  the minimum dee voltage required to clear the stripper foil shroud at the end of the first orbit after stripping is 45 kV. Scaling tests on 5.6 MeV/u Iodine beam suggest that adequate extracted beam current for the proposed physics experiment (5-10 nA) should be possible.

The details of the cyclotron have been described at earlier conferences in this series<sup>2</sup>. We will comment on our experience with some of the more novel machine features.

Table 3

Chronology. Commissioning of the Chalk River Superconducting Cyclotron	
1984 July-August	Extraction channel tests in special cryostat
September	Installation of extraction channel in cyclotron cryostat
October 31	Cyclotron cryostat moved to cyclotron vault
1985 January	Replacement of cryostat shield cooling manifolds
March	Cryostat installed in magnet yoke and cooled to 4.6 K
May	Magnet centering and calibration for commissioning beam
July 25	First charge state spectrum from injected $^{127}\text{I}$ beam
August	RF main tuner joints welded
September 10	First beam accelerated
September 12	Beam accelerated to 1.27 GeV at extraction radius (10 MeV/u)
November 14	Deflector installation completed
November 19	First extracted beam
1986 March 03	Beam to first nuclear physics experimental target
March 31	First attempt to accelerate with rf in $\pi$ -mode
May 12	Development of 710 MeV $^{127}\text{I}$ beam (5.6 MeV/u)
May 27	Second nuclear physics experiment starts
June 24	Exploratory tests for nuclear physics experiment #3
July-September	Various cyclotron, rf tests
September 22	Nuclear physics experiment #3 (5.6 MeV/u)
October	Development of 20 MeV/u $^{79}\text{Br}$ beam

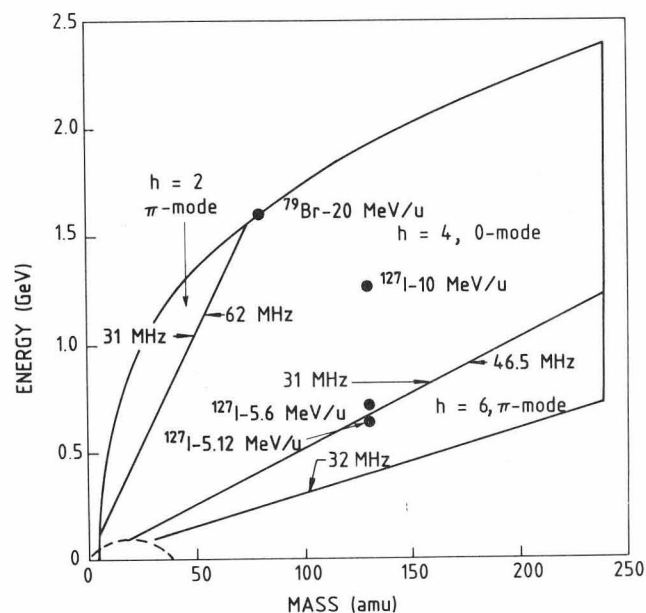


Fig. 4 Energy-mass limits of the Chalk River Superconducting Cyclotron.

#### Injection by Stripping

The Chalk River Superconducting Cyclotron is the first superconducting cyclotron to be injected from a Tandem Van de Graaff. The procedure for matching the beam from the tandem to the cyclotron optical properties and admittance was described in a paper at the 1985 Vancouver Accelerator Conference<sup>5</sup>. The procedure works well and achieves a satisfactory match in one iteration.

All injection trajectories pass through a common point and arrive at the fixed stripper azimuth over a range of radii from 145-265 mm. Foils, mounted in stainless steel frames, are inserted in copper shrouds carried on a chain mechanism from a magazine on top of the cyclotron to the required radial position inside the dee between hills 1 and 4. Changing a worn foil takes approximately one minute and generally requires no adjustment of the other cyclotron parameters.

When a new beam is developed the usual procedure is to inject the beam into the computed isochronous field, check its position at the two radial probes and then position the foil at its computed position. The required charge state is optimized for correct radius at the probes and the beam centred in the midplane using the four injection steerers.

The rf is then turned on, and usually a turn pattern is observed immediately.

#### Stripper Foil Behaviour

Two limiting cases of stripper foil behaviour have been noted with the two  $^{127}\text{I}$  beams developed. For the 10 MeV/u beam which is injected at 71 MeV, the foil thins. Over the average eight hour foil lifetime the peak of the charge state distribution moves slowly to lower charge and quite abruptly the current falls and evidence of a damaged foil appears (i.e., the probe detects beam at the unstripped beam location). For the 5.6 MeV/u beam, injected at 42 MeV, the current falls steadily over the four hour foil lifetime. In this case the fall off in current is due to loss in beam (and turn pattern) quality as the foil thickens and foil use is usually terminated when the current falls to 50% of the starting value. For  $^{127}\text{I}$ , 20 microgramme/cm<sup>2</sup> foils have been used. 10 microgramme/cm<sup>2</sup> foils break after one hour's use, or less, and are too thin to achieve equilibrium charge state distribution.

#### Isochronous Field

The isochronous field is set up using computed values of the field parameters. These are the currents in the outer and inner superconducting coil pairs (Fig. 5) and the axial position of the 13 sets of eight trim rods (Fig. 6).

The initial turn pattern obtained when the rf is turned on can be improved in definition, betatron oscillations minimized and beam intensity maximized, by minor adjustments to the injection steerers. Isochronism and centering are then corrected. The phase acceptance is plotted at low (200 mm) and high (600 mm) radii and the optimum phase found from energy focusing, i.e., radius of a given centered turn maximized.

Figure 7 shows a phase acceptance plot for  $^{127}\text{I}$ , 10 MeV/u, derived by measuring the integral probe current as a function of dee phase delay. One reason for the tails of the acceptance plot not spanning a full 180 degrees of phase is that the shroud of the stripper foil scrapes the beam for a turn separation less than 4 mm. The arrow shows the location of the optimum phase for energy focusing. Typically the low and high radius optimum phases may initially differ by up to 2 ns delay time which corresponds to a phase slip of 0.08% per turn for  $^{127}\text{I}$ , 10 MeV/u extraction energy. This is most readily corrected by an overall main field change of 0.08%. Changing the main coil currents takes one or two minutes, and is preferable to the more lengthy retuning of the rf amplifier and cyclotron tuners. We have not found it necessary to

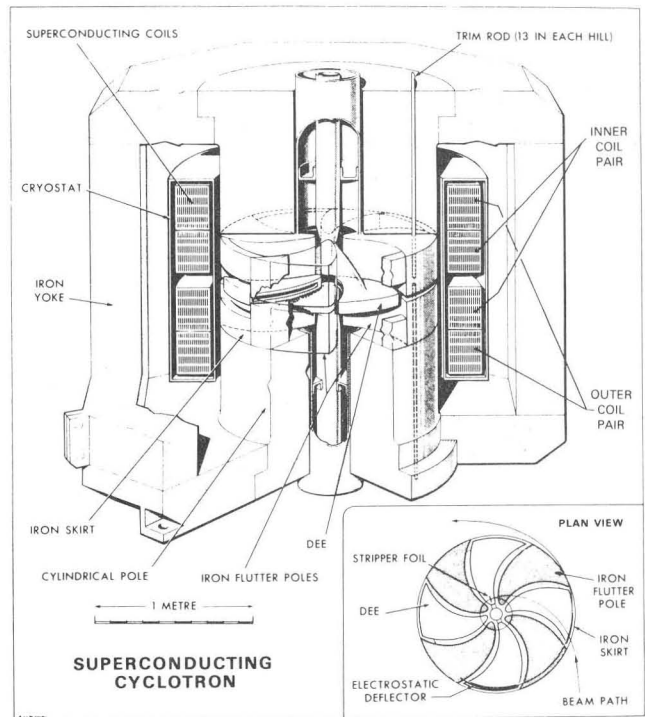


Fig. 5 Diagrammatic section of the Chalk River Superconducting Cyclotron.

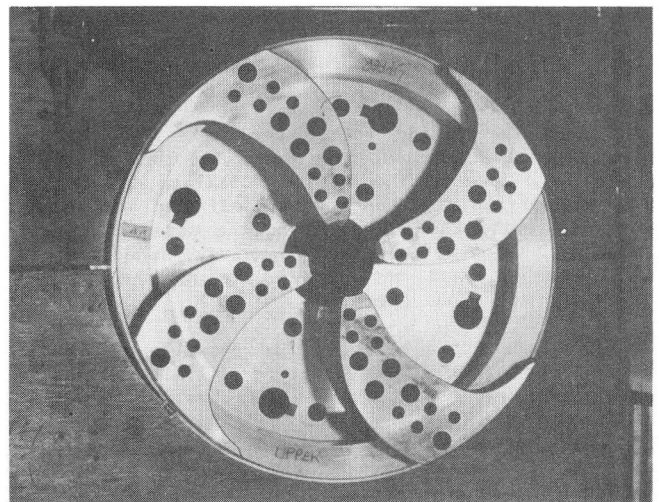


Fig. 6 Trim rod distribution in the steel poles.

adjust the main field tilt or the trim rods to isochronize the field, with beams developed so far, because computed settings combined with the repeatability of the magnet give an initial field very close to isochronism.

If a small injection steering adjustment with compensating foil position correction does not centre the orbits at low and high radii then it indicates that the energy of the injected beam does not match the isochronous field. Injection via a common point on the trajectory calls for precise setting of the injected beam energy. Adjustment of the injection beam line is a

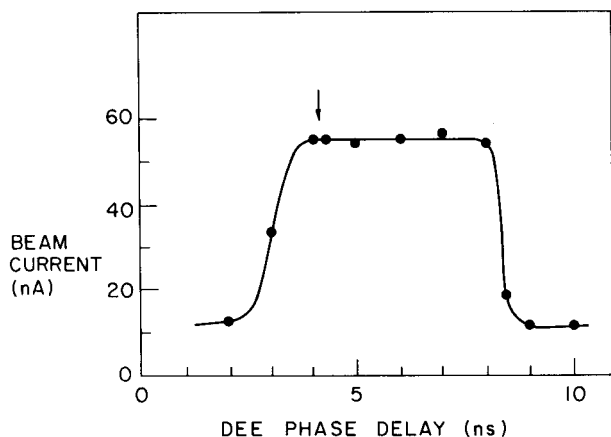


Fig. 7 Phase acceptance plot for  $^{127}\text{I}$ , 10 MeV/u. 1 ns corresponds to approximately  $15^\circ$  of rf phase angle.

lengthy procedure taking about an hour so the preferable procedure is to shift the isochronized field and radiofrequency together. After finding that for the first two beam set-ups the field and frequency had to be raised by 0.25% each time to centre the orbits the injection beam line analyzing dipole settings have been biased "permanently" to correct the apparent discrepancy between dipole and cyclotron field calibrations.

Once these small corrections have been made to the computed parameters a beam can be restored after a complete shutdown of the injection steerers and main magnet and rf system by simply resetting to the previous values, provided that ion source and tandem conditions have not been changed in the interim.

Figure 8 shows a typical turn pattern obtained from the two radial probes. Each probe has five fingers and an integral plate. In these plots the outputs from the five fingers are displayed. The axial pitch of the fingers is 4 mm and the exposed area is 1 mm in radial width. This pattern is for  $^{127}\text{I}$ , 10 MeV/u. The beam is 3-4 mm or less in axial extent and with 112 turns from injection to the extraction orbit the mean energy gain is 10.7 MeV per turn.

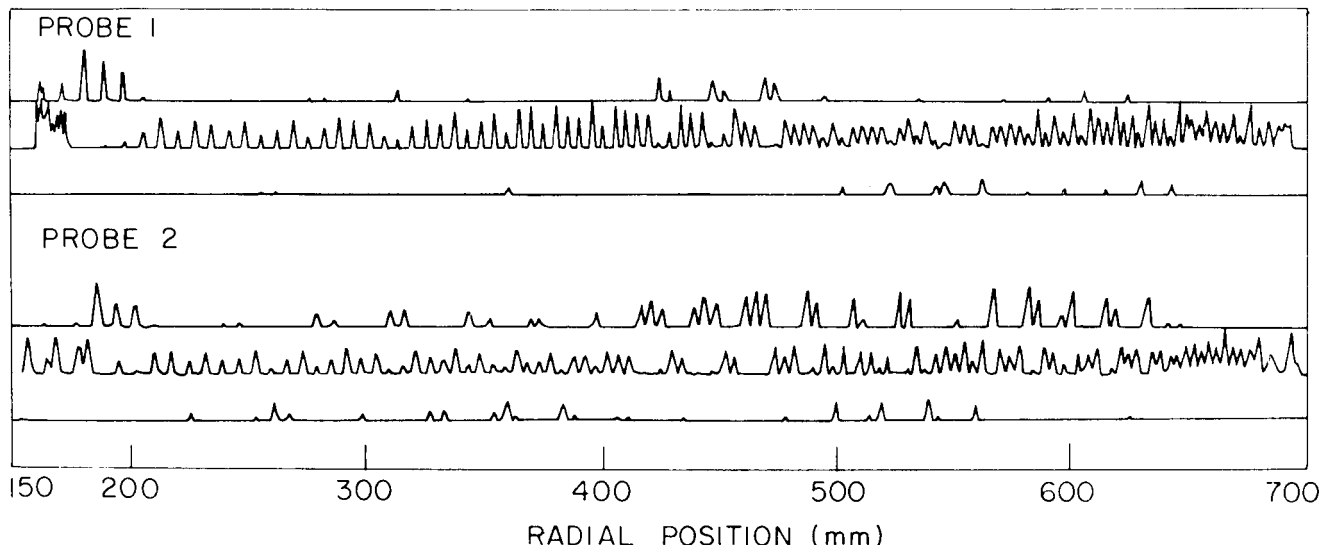


Fig. 8 Turn pattern for  $^{127}\text{I}$ , 10 MeV/u.

Figure 9 is the first 50 mm of a similar turn pattern showing the excellent radial width and turn separation after stripping and some of the unutilized charge states which are lost after a few turns.

The second turn suffers an axial deflection of 4 mm which is caused by an asymmetric rf electric field at the dee tip. Initially this led to an appreciable beam loss by scraping off on the foil carriage guides inside the dee. This loss has now been eliminated by adjusting the rf balance between the upper and lower dee pairs. The relative positions of the upper and lower tuners are adjusted until the beam current is maximized. As the balance is changed to drive the displaced turn down, the axial betatron amplitude increases so the balance is set 'down' just enough to avoid scraping the beam. The deflected beam returns to the midplane in one axial betatron period. The reason for the rf asymmetry may be related to the axial asymmetry of the electrical contact of the foil track to the dee but this has not been experimentally studied yet.

#### Trim Rods

Because the pole steel always operates fully saturated it is possible to trim the local field geometry (in a repeatable and reversible manner) by moving parts of the pole. We have chosen to use 13 axial rods, 40 mm and 60 mm in diameter, spaced across each pole face, 104 rods in all, for field trimming. There are no trim coils in the Chalk River Superconducting Cyclotron. A full description of the properties of the trim rods has been given elsewhere<sup>3</sup>. The contributions of the main coils and the trim rods to the midplane field are simply additive in all cases and as mentioned above, small adjustments to isochronism have not required any movement of the trim rods from their computed settings.

The trim rods were intended to be used mainly to adjust the value of the axial field component at the midplane and are thus normally moved in reflection symmetry about the midplane. In attempts to correct axial asymmetries in the beam orbits we have deliberately set some rod pairs asymmetrically relative to the midplane. This has the effect of introducing local radial and azimuthal fields without changes in the isochronous field to first order. The effect of the

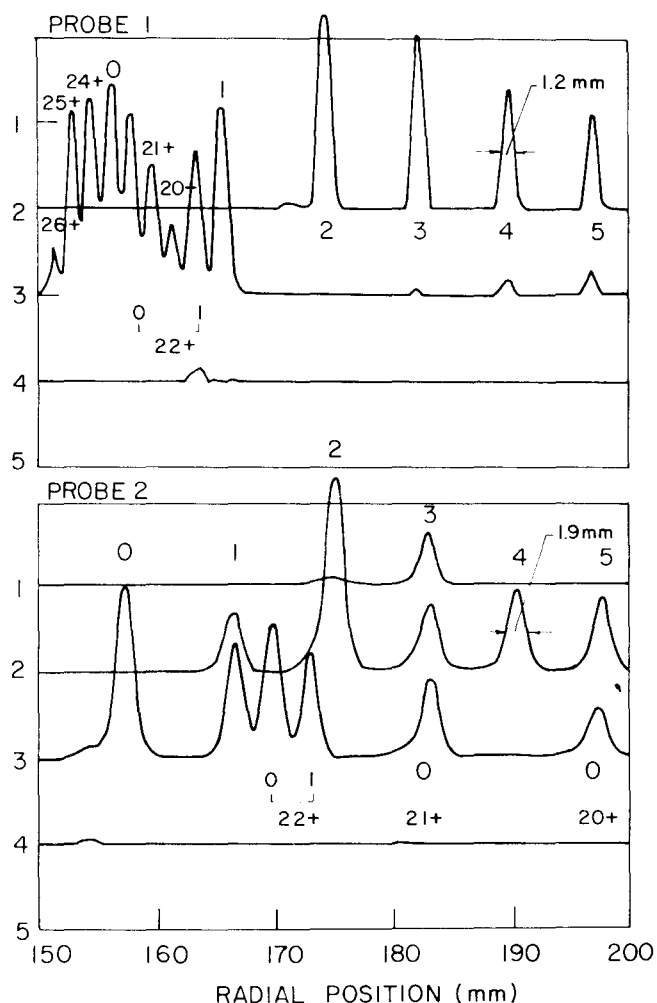


Fig. 9 Turn pattern for  $^{127}\text{I}$ , 10 MeV/u, inner radii.

perturbing fields on the orbits are as might be expected. The radial fields produce axial deflections and induce increased axial betatron oscillations. The effects of displacements of a set of rods at a given radius add 'arithmetically'. The effect of the radial fields at the outer edge of one trim rod radial set can be compensated by setting up radial fields with the next outer set, and so on to the outside. In this way a local radial field can be set up at any rod inner radial limit and the 'matching' field at the outer radial limit effectively compensated. No utility has been yet found for such field perturbations except that we were able to reduce a vertical (axial) displacement of the extracted beam by steering with the radial field of the #13 (outermost) trim rod set.

#### Extraction

The first harmonic field perturbation which decentres the outer orbits to increase the turn separation and steer the beam into the electrostatic deflector is set up by displacing the 13th trim rod in each hill from its isochronous setting (the rod movements are antisymmetrical so that the isochronism is not changed). A task is provided on the control computer to move the rods and the operator merely has to set the azimuth and amplitude of the harmonic at the control touch panel. A test of this system was carried out by comparing the turn separation of the last two turns at axial probe #2 with the turn separation computed by SUPERGOBLIN<sup>4</sup>. The experimental data for

a 0.75 mT harmonic amplitude are shown in Fig. 10. Computed turn separations for 0.75 mT and 1.0 mT at the same dee voltage show a comparable range and similar azimuthal dependence but vary about a different mean value. The degree of agreement is encouraging, and perhaps as much as can be expected. The data for the computation does not necessarily match the actual starting conditions of the real orbits in this case and orbit centre displacements comparable with the measured turn separations may exist between the measured and computed orbits.

The four channel currents, the deflector voltage and the magnetic first harmonic are set to values computed by SUPERGOBLIN. A split plate "stub" probe just following the deflector is used to "centre" the extraction trajectory by adjustments to the first harmonic amplitude and azimuth and the deflector voltage. The extracted beam current is then maximized by systematic small adjustments to all extraction parameters at the extraction channel exit, first using the retracted radial probe #1 and then at the first extraction beam line Faraday cup. If the orbits are centred within one or two millimetres and the beam equally divided on the stub probe plates, extraction channel optimization takes no more than a few minutes.

The extraction channel is quite small, the beam pipe in the channel 1 section has internal dimensions of 8 x 13 mm. These small dimensions are imposed by the space between the main coil supports at the mid-plane (80 mm) and the cross section of the superconducting windings in our initial channel design. The clearance between the beam pipe and the channel surface at 4.6 K is just over 2 mm. Further the present channel has some potential limitations because we put in abeyance the use of brittle niobium tin for the channel windings and used lower current niobium-titanium alloy. This implies that extraction in the low energy, low mass region of the mass-energy acceptance area of the cyclotron (see Fig. 4) may be difficult. The best transmission of the channel (relative to current on the stub probe) is about 80%. We have carried out scaling tests with the Iodine beam to define by how much a lost area in the energy-mass plane may be reduced if some transmission is sacrificed. A future upgrade of the cyclotron will include a redesigned channel if the channel proves to have operating restrictions.

The deflector system has been tested to 100% of its design rating of 140 kV/cm. An early limitation due to leakage through the cooling for the water resistor rf termination in the deflector high voltage feed has been overcome by maintaining the water resistivity at 16  $\text{M}\Omega\cdot\text{cm}$  or better. The 1 mA high voltage supply is marginal and will be upgraded to improve reliability.

Figure 11 shows the radial probe #1 trace at the crossing of the extracted trajectory. Here the axial extent of the beam (10 MeV/u,  $^{127}\text{I}$ ) is 3 mm with a FWHM of 6 mm. For beams developed so far, the extracted beam leaves the magnetic channel below the midplane. In this example the beam is 3 mm below the centre of the probe. To cope with this unanticipated vertical displacement an extra vertical steerer had to be added to the extraction beam line. Space for a temporary steerer was found between the object slits SE-1 and the lens QE-2 (see Fig. 2), but a specially designed X-Y steerer is under construction to fit in front of lens QE-1, in place of the existing horizontal steerer.

Table 4 shows some transmission coefficients for the 10 MeV/u,  $^{127}\text{I}$  beam through the combined injector and cyclotron system.

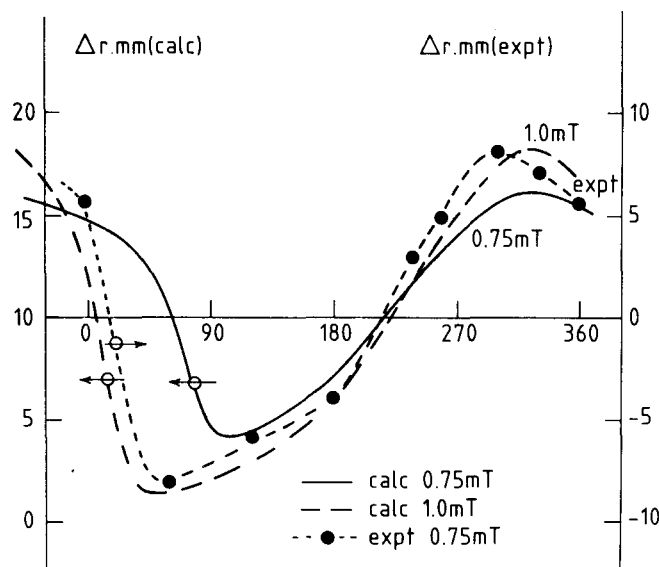


Fig. 10 Turn separation as a function of first harmonic azimuth. Computed values for dee voltage of 60 kV.

Operating Record

Since 1986 February when we first began to extract beam reliably the cyclotron has been operated for a total of fourteen weeks including delivery of beam for three nuclear physics experiment series.

Although the cryogenic and magnet systems are fully protected against component failure and operator error by hardware interlocks we have not yet put in operation intelligent microprocessor driven controllers to handle automatic start-up and shut-down for these systems. Consequences of power outage for example, must be dealt with by human operators. Twenty-four hour a day operation under these limitations would be an intolerable strain on our manpower resources and so, cyclotron operation has been on a basis of daily start-up and sixteen hours running per day, giving up to 12 hours of useful target beam time per day. Correcting this situation and attaining twenty-four hour per day operation is our highest priority.

Table 5 gives an approximate breakdown of system utilization by week over the 35 week period from February 1.

As might be expected, the most extensive cause for system unavailability comes from the helium liquefier. Maintenance requirements are now better understood and this should result in an overall improvement in availability. The "hours possible" assume a 5-day week and 16 hours a day operation.

Commissioning has uncovered some limitations in parts of the cyclotron. Due to vacuum instability the rf accelerating system cannot be operated continuously at full power at the highest frequency at present. An accident with a jammed gate valve in the foil changer caused damage to the thermal insulation of one cryopump when the midplane vacuum was partially vented with the cryopumps full. Although we are operating with one cryopump at present, which is adequate at 32 MHz up to 95 kV dee voltage and up to 60 kV at 60 MHz, the vacuum instability does not appear to be simply a problem of pumping speed or pump outage but related to rf leakages into the cryopumps and temperature drifts of the thermal baffle which is cooled by helium boil-off. A modified cryopump design is under development to overcome these deficiencies.

The foil changer operated smoothly for nine months, but then developed some stiffness in the transport chain which led to shroud misalignment and consequent jamming and minor damage to the changer mechanism during foil changing. We believe that this is a vacuum lubrication problem probably soluble by regular maintenance.

We have not been able to operate the rf system in the  $\pi$ -mode, which is required for the highest energies (above 21.5 MeV/u) and for the lowest energies (below 5.2 MeV/u), because of excessive wall heating in the cryostat near the midplane. In development tests, before the extraction lenses and probe ports were added to the cryostat wall, operation in  $\pi$ -mode presented no problems. It is expected that straightforward corrections to the rf shielding in these regions will overcome this problem.

Vacuum leaks have developed at seals in the moving parts of rf tuners and trimmers over several months of operation. Designs of these components are being modified but this in any case is a problem amenable to routine maintenance.

Beam Quality

The original specification for the cyclotron called for an energy resolution of 5 parts in  $10^4$ . The beam pulse width arriving at the target location as measured by time distribution of gamma rays detected by a plastic scintillator indicates an energy resolution better than 8 parts in  $10^4$ . This result includes possible contributions from dispersive elements in the beam line and inherent broadening from the scintillator and electronics which could account for half the measured width. The measurement was made on the 5.6 MeV/u iodine beam.

The emittance of the beam circulating in the cyclotron can be estimated as about  $0.7 \pi \text{ mm} \cdot \text{mrad}$  in both axial and radial transverse planes at the extraction radius for 50 nA of  $^{127}\text{I}^{23+}$  at 10 MeV/u.

Concluding Summary

The Chalk River Superconducting Cyclotron has accelerated Iodine ion beams to 0.71 GeV and 1.27 GeV and these beams have been extracted and delivered to a target for nuclear physics experiments. The choice of initial beams developed was made to minimize complications in operating the cyclotron, and we have been able to show that the novel concepts of the machine including the superconducting main and extraction fields, trim rods, the dee system and the injection from a Tandem, all operate harmoniously, and as intended. Figure 12 shows the cyclotron installed in its shielded vault.

During development without beam the magnet system was operated to full power and the rf system to full power in a vacuum test chamber at all frequencies and both modes. The rf system has now been run at the lower end of the frequency range to almost full power, while incorporated in the cyclotron.

We are now turning our attention to the priorities of nuclear physics users and their requirements will give us the opportunity to move some machine parameters towards specification limits. For example the 20 MeV/u  $^{79}\text{Br}$  beam now being developed requires rf operation close to the upper frequency limit and 80% of full voltage on the electrostatic deflector, and high voltage on the dees is preferred.

Most of the beams of current nuclear physics

Table 4

<sup>127</sup>I 10 MeV/u Beam Transmission

	Charge	Energy	Beam Current		
			(nA)	(pA)	Transmission
From Ion Source	-1	200 keV	1700	1700	2.7%
From Tandem (buncher off)	7+	70.9 MeV	320	46	50%
From Tandem (buncher on)	7+	70.9 MeV	160	23	15%
After Stripper in Cyclotron	23+	>70.9 MeV	(80)	3.5	(100%)
At Entrance to Electrostatic Deflector	23+	1.27 GeV	80	3.5	74%
Through Electrostatic Deflector	23+	1.27 GeV	60	2.6	92%
Through Extraction Channel	23+	1.27 GeV	56	2.4	83%
On Cup before Target	23+	1.27 GeV	46	2.0	

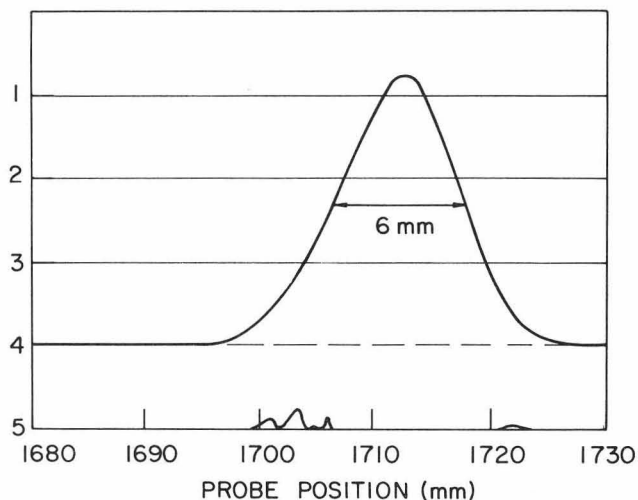


Fig. 11 Radial profile of extracted beam.

Table 5

Cyclotron Utilization, February - September 1986

By week	Weeks
Cyclotron development - operation	9
Operation of rf and vacuum system for tests	7
Beam output for nuclear physics experiments	5
Total useful operation	21
Cyclotron not available:	
Helium liquefier maintenance	3
Low liquid helium production	4
Injector problems	1
Midplane inspection after $\pi$ -mode tests	2
Breakdown from external causes	2
Miscellaneous	2
Weeks available	21
Weeks not available	14
Total	35
By hours	
Possible hours of operation	2800
Hours of operation with beam	500

interest, e.g., 45 MeV/u carbon and beams around 5 MeV/u for nuclear reactions involving fusion, require operation in the  $\pi$ -mode and successful commissioning for operation in this mode is now a high priority.

References

1. W.G. Davies, Proc. 10th Int. Conf. on Cyclotrons and their Applications, East Lansing, Michigan, 1984, p. 328 (IEEE Catalog No. 84CH1996-3).
  2. J.H. Ormrod, et al., Proc. 10th Int. Conf. on Cyclotrons and their Applications, East Lansing, Michigan, 1984, p. 245 (IEEE Catalog No. 84CH1996-3).
- See also J.A. Hulbert, et al., IEEE Trans. Nucl. Sci., NS-32 (1), 2643 (October 1985).
3. J.H. Ormrod, et al., IEEE Trans. Nucl. Sci., NS-26 (2), 2034 (April 1979).
  4. E.A. Heighway and C.R. Hoffmann, IEEE Trans. Nucl. Sci., NS-32 (1), 2522 (October 1985).
  5. W.G. Davies, IEEE Trans. Nucl. Sci., NS-32 (2), 2757 (October 1985).

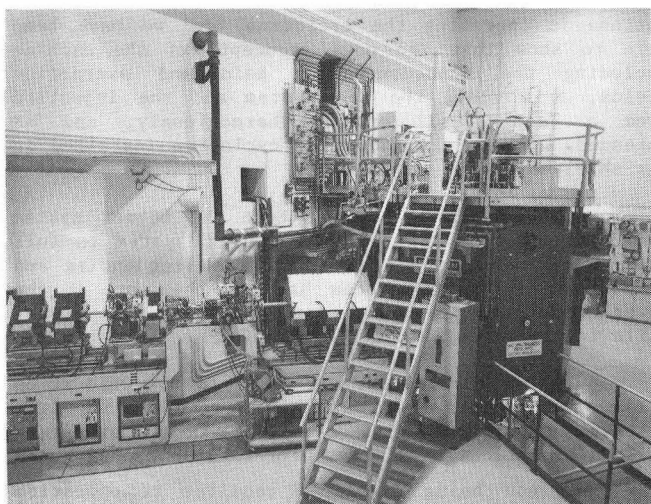


Fig. 12 The cyclotron in its vault.